

3-D Soil Stratification Methodology for Geoelectrical Prospection

Wesley Pacheco Calixto, *Member, IEEE*, A. Paulo Coimbra, *Member, IEEE*, Bernardo Alvarenga, Jose Paulo Molin, Alexandre Cardoso, and Luciano Martins Neto

Abstract—The purpose of this paper is to present an innovative methodology for 3-D soil stratification based on geoelectrical prospection. This methodology is useful in optimal substation grounding system designs by providing an accurate 3-D soil resistivity model. In the present methodology, the area being studied is subdivided into squared subareas and a recently developed geoelectrical prospection method based on the Wenner’s method and on a genetic algorithm is applied to each subarea’s edge. For each subarea, the soil stratification result consists of the number of layers and of its electrical resistivities and thicknesses. A global 3-D soil stratification solution is then obtained from these data. Results obtained with this new method are presented and discussed.

Index Terms—Grounding systems, inverse problems, 3-D soil stratification.

I. INTRODUCTION

THERE ARE a wide variety of geoelectrical prospecting methods, most of which are not well known nor widely applied, except for some procedures that have achieved a widespread maturing on the practical aspects [1], [2]. Moreover, it should be noted that the various methods are independent techniques but they are all derived from the same model, whose solution is needed to interpret measurements of potential difference V , corresponding to a flow of current I injected through the existing geological structures *in loco* [3], [4].

These geological structures significantly affect electrical grounding systems. The soil chemical composition varies over time, being closely linked to the weather, causing uncertainty

Manuscript received November 10, 2011; revised February 17, 2012; accepted March 25, 2012. Date of publication June 12, 2012; date of current version June 20, 2012. This work was supported by the CAPES Foundation, Ministry of Education of Brazil. Paper no. TPWRD-00964-2011.

W. P. Calixto is with the Nucleus of Research and Extension in Sustainable Process Technology, Electrotechnical Department, Federal Institute of Goias (IFG), Goiania 74055-110, Goias, Brazil, and also with the Institute of Systems and Robotics (ISR), University of Coimbra, Coimbra 3030-290, Portugal (e-mail: wpcalixto@ieec.org).

A. P. Coimbra is with the Institute of Systems and Robotics (ISR), University of Coimbra, Coimbra 3030-290, Portugal.

B. Alvarenga is with the Electrical and Computer Engineering School, Federal University of Goias (UFG), Goiania 74605-010, Goias, Brazil.

J. P. Molin is with the University of São Paulo (USP), Luiz de Queiroz College of Agriculture (ESALQ), Piracicaba 13418-900, São Paulo, Brazil.

A. Cardoso and L. M. Neto are with the Nucleus Research and Development, Department of Electrical Engineering, Electromagnetism and Electric Grounding Systems, Federal University of Uberlandia (UFU), Uberlandia 38400-902, Minas Gerais, Brazil.

Color versions of one or more of the figures in this paper are available online at <http://ieeexplore.ieee.org>.

Digital Object Identifier 10.1109/TPWRD.2012.2193602

on the value of the electrical resistivity and eventual changes in the electrical parameters of the grounding system [5], [6]. This uncertainty in each soil layer resistivity is a major problem in designing an electrical grounding system and even through field tests, there is no guarantee that it will remain stable over time [7], [8]. To understand how the geologic structure of a particular location affects the design of an electrical grounding system, it is necessary to know the soil structure and its composition [9].

The geoelectrical prospecting methods are practical applications of Maxwell’s equations, which enable obtaining the apparent resistivity curve, raised experimentally by measurements *in loco*. This curve is the basis of all methods of soil stratification in layers of different electrical resistivity [10].

The model of parallel homogeneous layers meets the need for electric grounding designs, giving a qualitative and sometimes quantitative insight of the soil structure and its electrical properties. There will always be uncertainty about the measurement of the electrical resistivity of the soil, because the model of homogeneous horizontal layers does not always correspond to the real geological formation [3], [6], [9].

With an accurate soil stratification model, it is possible to develop safer electrical grounding systems. This paper presents a new method for 3-D geoelectrical stratification of the soil in multiple horizontal layers. This new method is more accurate than traditional methods [9], because the soil is characterized in three dimensions, increasing the resolution of the electrical properties of the soil model.

The basic idea of the proposed methodology is to divide a large area into several subareas, in order to “discretize” the stratification and decrease the uncertainty of the soil layers resistivity and thickness. The analysis of results confidence obtained from the 3-D stratification makes it possible to identify areas in a substation where depth, spacing, and thickness of conductors should be changed in order to improve the grounding grid design.

In Section II, some mistakes associated with the traditional methods are discussed. In Section III, the direct and inverse processes of horizontal soil stratification are described and the new method for 3-D stratification is shown. Section IV presents the obtained results and, finally, Section V presents the conclusions.

II. CONSIDERATIONS AND SOME COMMON MISTAKES INHERENT TO GEOELECTRICAL PROSPECTION

The Wenner’s method is the usual performed test to collect field data. It is accepted that in homogeneous soils, the electric current injected through the outer electrodes flows down to a depth of the order of magnitude of the electrodes spacing. Therefore, for homogeneous soils, the depth of stratification is

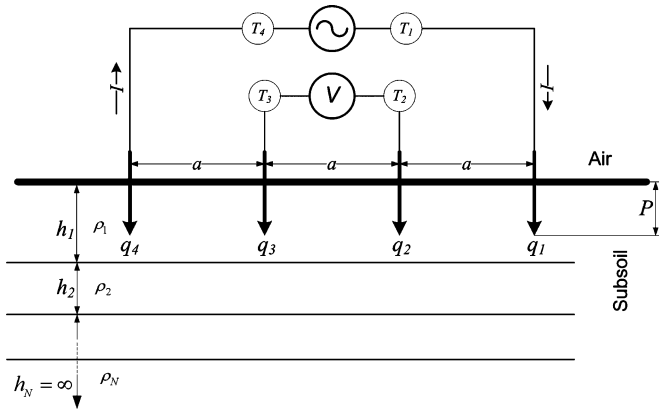


Fig. 1. Representation of a soil with homogeneous layers being analyzed with the Wenner’s method and equivalent concentrated parameters of the resistance of the soil.

approximately $3 \cdot a$. On the other hand, in the case of heterogeneous soils, this idea does not hold, for the current penetration will depend on other factors.

Soils with higher humidity content have lower electrical resistivity. The electric current I may be conducted through wet soil in two main ways [11]. One way is the interstitial water which contains dissolved electrolytes. Another way is through mobile cations that exist near the surface of the soil particles that are electrically charged. These cations react chemically with the water, producing new chemical elements that are more electrically conductive. This effect, in acid soils ($pH < 7$), is very important and is responsible for a huge variation of the electrical resistivity with the humidity of that soil. If the soil is alkaline ($pH > 7$), the soil humidity variation has little effect on the value of the soil electrical resistivity. For this reason, it is then very important to know the soil pH for grounding design purposes.

The Wenner method and the soil hypothetical model are illustrated in Fig. 1. Current injection electrodes and voltage measurement electrodes of length P [m] are equally spaced by a distance a [m]. The soil is considered to have N homogeneous layers. The i th soil layer has thickness h_i [m] and resistivity ρ_i [$\Omega \cdot m$]. The N th layer has infinite thickness. The apparent soil resistivity curve $\rho_{aE}(a)$ [$\Omega \cdot m$] is given by [3], [5], [6]

$$\rho_{aE}(a) = \frac{4\pi a \cdot R_m}{1 + \frac{2a}{\sqrt{a^2 + 4P^2}} - \frac{2a}{\sqrt{4a^2 + 4P^2}}} \quad (1)$$

where R_m has a dimension of resistance and represents the quotient of measured voltage V by injected current I in the Wenner arrangement—Fig. 1. The first mistake in interpreting the Wenner method’s results is concerned with R_m . Since it is not possible to measure the voltage in the points of current injection or to inject current in the points of voltage measurement, R_m is defined as an apparent resistance and its definition should not be confused with Ohm’s concept of resistance.

Another common problem occurs in determining the resistivity of the first layer ρ_1 . The methods usually employed extrapolate the experimental curve of $\rho_{aE}(a)$ for $a = 0$. When the curve $\rho_{aE}(a)$ does not have a smooth behavior, the extrapolation leads to a wrong prediction of the resistivity of the first

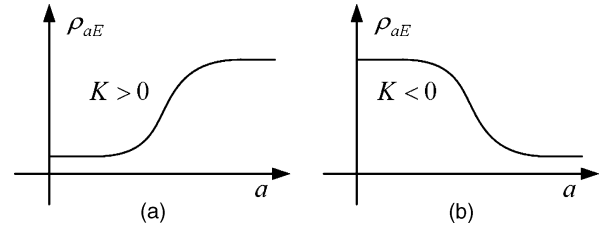


Fig. 2. Curves $\rho_{aE}(a)$ for soils with two or more layers i , with different reflections coefficient K . (a) ρ_i always increasing. (b) ρ_i always decreasing.

layer. Purely mathematical methods do not take into consideration the physical characteristics of the soil and its resistivity measuring system. Even a small error in ρ_1 propagates into the rest of the stratification. An unacceptable error in the value of ρ_1 fatally invalidates the rest of the soil stratification results.

When the soil has more than two layers, other problems arise. Indeed, the geoelectrical prospecting methods reported in the literature, from the more complex to the more simple ones, such as the graphics method, all produce significant errors [11]–[13]. The existing methods are based on the experimental apparent resistivity curve $\rho_{aE}(a)$ for two layers. The problem with these methods is the fact that they assume that experimental apparent resistivity curves $\rho_{aE}(a)$ with one inflection point corresponding to soils with only two layers [1], [3], [6].

The curves shown in Fig. 2 represent two-layer soils. In this figure, K is the reflection coefficient, defined by

$$K = \frac{\rho_2 - \rho_1}{\rho_2 + \rho_1}. \quad (2)$$

Although two-layer soils can be represented by the curves in Fig. 2, the opposite is not always true (i.e., such curves do not necessarily represent two-layer soils). This is easy to understand assuming, for example, a soil consisting of three or more layers, in which resistivities grow from the first to the last layer. In this case, the apparent resistivity $\rho_{aE}(a)$ is a monotonically increasing function as the curve shown in Fig. 2(a). Also, the curve in Fig. 2(b) is a monotonically decreasing function, which could represent a soil consisting of three or more layers, in which resistivities decrease from the first to the last. As a consequence, the number of inflections of the curve $\rho_{aE}(a)$ are not always associated with the number of layers N . On the basis of this consideration, by interpreting the curves $\rho_{aE}(a)$ of Fig. 2 as corresponding to a stratified soil with only two layers, a significant modeling error may be committed. In this paper, this curve interpretation error is called the *a priori* error.

Another mistake is inherent to the fact that the adopted soil model does not correspond to the real soil geological formation. The horizontal layers model is not true, for example, for a soil having a vertical crack. This situation is not predicted by the traditional stratification analysis.

It is important to note that in developing any mathematical or computational model to stratify the soil, the input data to the problem are just the values of the experimental curve $\rho_{aE}(a)$. The results to be obtained are the number of layers N , the i th layer resistivity ρ_i , and thickness h_i . For the N th layer, h_N is

considered to be infinity. The problem is then mathematically defined as

$$\rho_{aE}(a) \rightarrow N, \rho_i, h_i. \quad (3)$$

A well-known soil stratification method that does not avoid the *a priori* error because it assumes that increasing and decreasing sections of the curves $\rho_{aE}(a)$ of Fig. 2 correspond to two layers soil stratification is based on (4), [1], [3], and [6]

$$\rho_{aE}(a) = \rho_1 \cdot \left[1 + 4 \cdot \sum_{n=1}^{\infty} Q_n \right] \quad (4)$$

where Q_n is given by

$$Q_n = \frac{K^n}{\sqrt{1 + (2n \cdot \frac{h_1}{a})^2}} - \frac{K^n}{\sqrt{4 + (2n \cdot \frac{h_1}{a})^2}} \quad (5)$$

where h_1 is the thickness of the first layer, see Fig. 1.

One form of stratification proposed by Sunde [6] can be obtained by

$$\rho_{aT}(a) = 2\rho_1 \cdot a \cdot \int_0^{\infty} N_N(m) \cdot [J_0(ma) - J_0(2ma)] dm \quad (6)$$

where N_N is the characteristic function that defines the heterogeneous soil structure and J_0 is the Bessel function of order zero.

Equation (6) is a result of the propagation of the current density field through successive layers of different resistivity. N_N is required to calculate the apparent resistivity curve corresponding to an already stratified soil and combines transmission coefficients on the boundary between layers. N_N is univocally determined by the thicknesses, resistivities, and number of layers [9]. While (4) is specifically applied to two-layer soils, (6) is valid for soils of any number of layers.

III. METHODOLOGY

When solving problems by direct methods (direct problem), analytical or numerical techniques can be used. The solutions are the effects which are calculated based on the full description of its causes [15]. For soil stratification, the direct problem can be mathematically described by

$$\text{Direct Problem : } N, \rho_i, h_i \rightarrow \rho_{aT}(a). \quad (7)$$

In the proposed methodology, the direct problem seeks the theoretical curve $\rho_{aT}(a)$ using Sunde's formulation (6). The technique involves the calculation of the transmission coefficients T_i and the reflection coefficients KL_i for the i th layer, as illustrated in Fig. 3.

The inverse problem consists in finding possible causes (unknown) based on the observation of its effects (known) [16]. In the case of the soil stratification problem, the observed effect (known) is the experimental curve $\rho_{aE}(a)$ and the causes (unknown) are the number of layers N , the resistivity ρ_i , and the

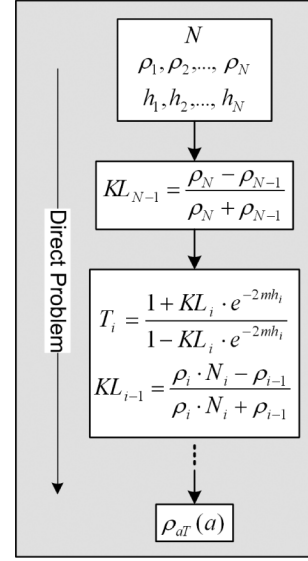


Fig. 3. Soil stratification direct problem (Sunde's algorithm—partial).

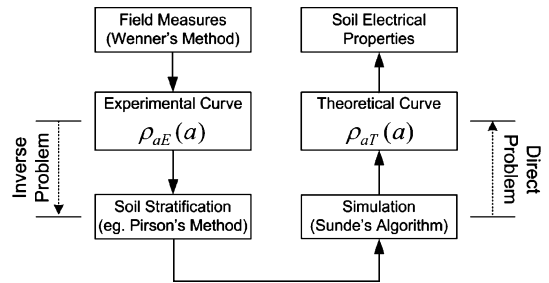


Fig. 4. Soil stratification process (direct and inverse problems).

thickness h_i of the i th layer. The inverse problem is then mathematically described by

$$\text{Inverse Problem : } \rho_{aE}(a) \rightarrow N, \rho_i, h_i. \quad (8)$$

Fig. 4 illustrates the direct and inverse problems applied to the process of soil stratification.

A. Genetic Algorithm (GA)

To solve the inverse problem, a GA is used, which is a heuristic iterative optimization method. The first population of the iterative process is obtained from an individual which is given by a first trial stratification using, for instance, Pirson's method [17]. This individual has the information of the first trial number of layers N , resistivity ρ_i , and the thicknesses h_i of each layer [9].

In this paper, the GA used is a real-coded GA [18]. The population is fixed with 20 individuals and the method of selection is the tournament. Two genetic operators are used: simple crossover and nonuniform mutation [19]. The population is divided into two parts, a population of resistivities and the other is thicknesses, which come together to be evaluated. The crossing rate R_C is $70\% \geq R_C \geq 20\%$ and the rate of mutation R_M , is $1\% \leq R_M \leq 30\%$.

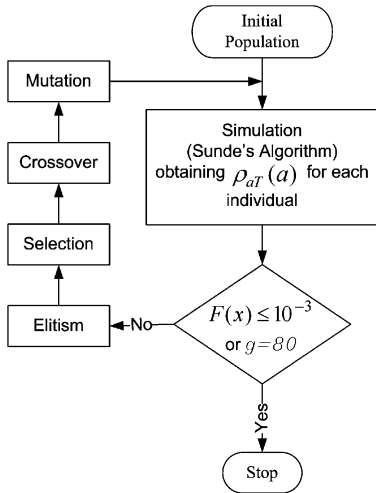


Fig. 5. GA iterative process.

In order to compute the fitness of the individuals of the generation under study, the direct problem is applied to each individual, and theoretical curves $\rho_{aT}(a)$ are obtained. These curves are then compared with the experimental curve $\rho_{aE}(a)$ with the use of the evaluation function $F(x)$ given by

$$F(x) = \sum_{i=1}^k \left| \frac{\rho_{aE_i} - \rho_{aT_i}}{\rho_{aE_i}} \right| \quad (9)$$

where k is the number of times the Wenner's method is applied at that location, that is, the number of known points of the curves $\rho_{aT}(a)$ and $\rho_{aE}(a)$. The process is repeated iteratively until one of the stopping criteria are satisfied. Two criteria are used as follows.

- 1) The fitness of the population is less than a certain target value (in this paper, $F(x) \leq 10^{-3}$).
- 2) The number of generations g is too large (max $g = 80$).

The GA iterative process is illustrated in Fig. 5. Each new population is generated using crossover and mutation operators [9], [20].

B. Practical Procedures

In order to obtain a 3-D soil stratification, the area to be stratified is subdivided into smaller subareas of $M \times M$ meters, as shown in Fig. 6. The Wenner's method is then applied at each edge of the subareas. In the cases presented in this paper, four measurements are performed in each side of the square areas. For each measurement, the chosen spacing between electrodes is 0.3, 0.5, 0.9, and 1.5 m. These values of a are chosen in order to validate the proposed method. However, a deeper stratification can be obtained by increasing the spacing between electrodes. . .

The number of times the Wenner's method is to be performed is given by

$$T(t, d) = 2(t \cdot d) + t + d \quad (10)$$

where d and $t \in \mathbb{N} | d = L/M$ and $t = C/M$. L and C are the width and length of the area to be stratified, as shown in Fig. 6. Note that L and C should be multiples of M .

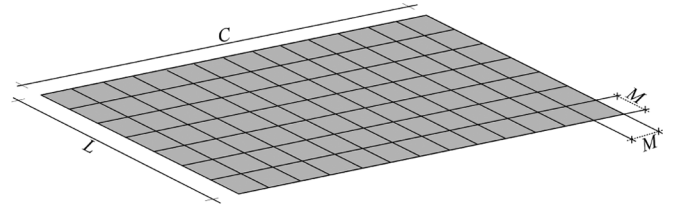


Fig. 6. Subdivision (discretization) of the chosen area for the stratification.

Thus, each subarea edge is then stratified considering the soil constituted by homogeneous layers, and the parameters N , ρ_i and h_i are calculated for all edges [21].

Each subarea is attributed to its own stratification parameters (N , ρ_i , and h_i) by averaging the parameters of its four edges stratification. For visualization purposes, the results obtained for the thicknesses of the layers in contiguous subareas are interpolated. In this paper, a cubic spline surface interpolation is used. The control points of the splines are taken at the edges of each subarea.

At the end of the 3-D stratification process, a representative resistivity $\bar{\rho}_i$ and thickness \bar{h}_i are assigned to each (global) layer corresponding to the mean values of the resistivity ρ_i and thickness h_i of each layer of all subareas. These values can be presented in a table or graphical form. It is also useful to present the sample standard deviations of the resistivities and of the thicknesses to quantify the dispersion of these values in the different subareas.

It should be emphasized that the method proposed enables inferring the layering of the soil down to a depth larger than the Wenner's method electrode spacing by using several measures (a number greater than the number of layers) with different electrode spacings and by considering a physical model with such layering (with Sunde's algorithm). The mean errors found in the studied stratifications are less than the mean errors obtained when considering only a two-layer stratification.

The evaluation function is the error to be minimized in the optimization process. This error quantifies the quality of the stratification obtained [9]. For each global stratification studied, E_T is also presented, the mean error found in the global stratification process of all the subareas, which corresponds to the mean of the differences $F(x)$ calculated for all edges

$$E_T = \sum_{i=1}^{d+1} \sum_{j=1}^{t+1} F(x_{ij}) \cdot \frac{1}{T(t, d)}. \quad (11)$$

IV. RESULTS

Since the proposed method utilizes the Wenner method, the limiting in the depth is given by the distance between the current electrodes. The places where the stratifications were made belong to electromagnetism and electric grounding systems nucleus research and development and are intended solely for conducting scientific research. Four different case studies are presented here.

The first study concerns an area of 13.5×13.5 m and the second study is an area of 22.5×22.5 m. The third and fourth studies were conducted in two areas of 36×36 m. In all four case studies, the subareas consisted of squares with $M = 4.5$ m.

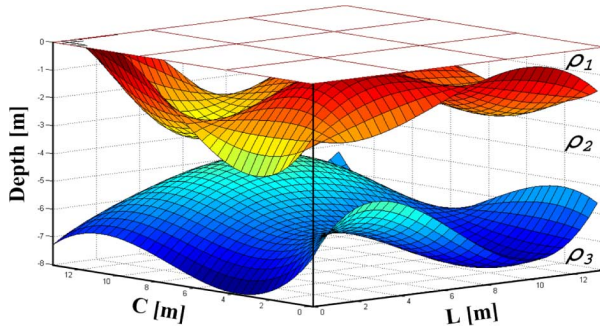


Fig. 7. First case 3-D interpolated stratification surfaces.

TABLE I
FIRST CASE STRATIFICATION RESULTS

Layer (i)	$\bar{\rho}_i$ [$\Omega \cdot m$]	SSD $\sigma(\rho_i)$	\bar{h}_i [m]	SSD $\sigma(h_i)$	\bar{d}_i [m]	SSD $\sigma(d_i)$
1	744	20.2	1.75	0.17	1.75	0.17
2	215	8.3	4.13	0.63	5.88	0.48
3	513	6.4	∞	—	∞	—

The results of the stratification process are presented in 3D plots where the depth is represented in a color scale. A discussion of the results is presented. For each stratification case, a table is presented with the representative (mean) resistivity value $\bar{\rho}_i$ and thickness \bar{h}_i of each layer and their sample standard deviations (SSD) [22], $\sigma(\rho_i)$, and $\sigma(h_i)$, respectively. These values quantify the dispersion of the resistivity and thickness of each layer among several subareas. Also, some applications present the mean depths (\bar{d}_i) of the layers separation surfaces and their sample standard deviations $\sigma(d_i)$.

A. First Case Study

In the first case study, the analyzed area is divided into nine subareas and the resistivity is measured in 24 locations over the subareas edges, according to (10). In each location, four measures are taken for different rod distances, using the Wenner's method (0.3, 0.5, 0.9, and 1.5 m). The stratification obtained consisted of three layers separated by the curved surfaces shown in Fig. 7. The representative parameters (result) of the stratification are shown in Table I. E_T , the mean error found in this global stratification, is equal to 3.51%.

B. Second Case Study

In the second case study, the analyzed area is partitioned into 25 subareas and the resistivity is evaluated in 60 locations. The obtained stratification consists of three layers, separated by the surfaces shown in Fig. 8. The parameters of the stratification are shown in Table II. The mean error E_T is equal to 3.16%.

C. Third Case Study

The analyzed area is divided into 64 subareas for the third case study, and the resistivity is measured in 144 locations. The stratification solution consisted of three layers. The surfaces that separate the layers are shown in Fig. 9. The parameters of

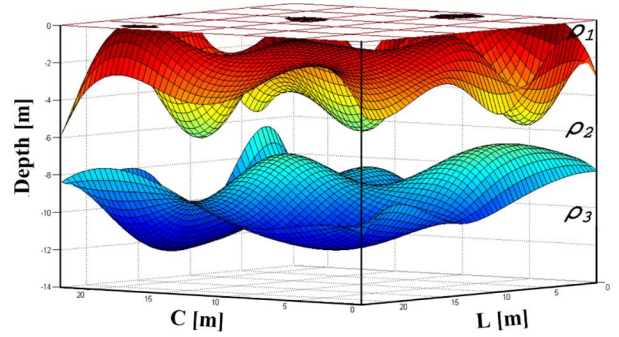


Fig. 8. Second case 3-D interpolated stratification surfaces.

TABLE II
SECOND CASE STRATIFICATION RESULTS

Layer (i)	$\bar{\rho}_i$ [$\Omega \cdot m$]	SSD $\sigma(\rho_i)$	\bar{h}_i [m]	SSD $\sigma(h_i)$	\bar{d}_i [m]	SSD $\sigma(d_i)$
1	1047	24.6	2.32	0.60	2.32	0.60
2	1848	34.0	7.05	0.79	9.37	0.28
3	11109	136.1	∞	—	∞	—

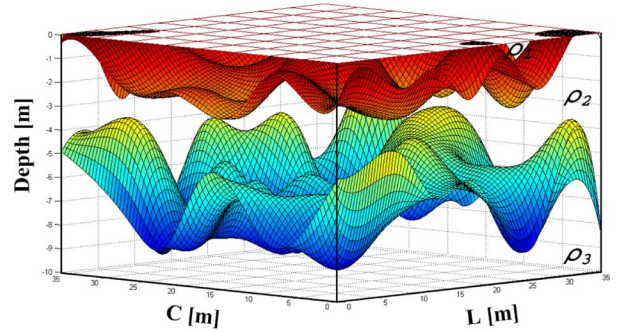


Fig. 9. Third case 3-D interpolated stratification surfaces.

TABLE III
THIRD CASE STRATIFICATION RESULTS

Layer (i)	$\bar{\rho}_i$ [$\Omega \cdot m$]	SSD $\sigma(\rho_i)$	\bar{h}_i [m]	SSD $\sigma(h_i)$	\bar{d}_i [m]	SSD $\sigma(d_i)$
1	627	12.8	1.45	0.19	1.45	0.19
2	471	31.5	5.03	0.47	6.48	0.30
3	317	7.2	∞	—	∞	—

the stratification are shown in Table III. For this case, $E_T = 11.12\%$.

D. Fourth Case Study

Here, the analyzed area is also divided into 64 subareas. The resistivity is evaluated in 144 locations. The stratification obtained consists of four layers. The separate surfaces are shown in Fig. 10, and stratification parameters are shown in Table IV. For case IV, $E_T = 2.85\%$.

E. New Ways of Displaying Stratification Results

Fig. 11 presents the stratification results of the four cases, allowing an easy comparison of several global stratifications. The diagrams show white lines that indicate SSD at each separation

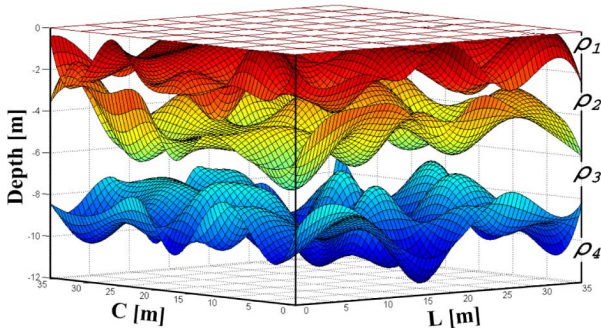


Fig. 10. Fourth case 3-D interpolated stratification surfaces.

TABLE IV
FOURTH CASE STRATIFICATION RESULTS

Layer (i)	$\bar{\rho}_i$ [$\Omega \cdot m$]	SSD $\sigma(\rho_i)$	\bar{h}_i [m]	SSD $\sigma(h_i)$	\bar{d}_i [m]	SSD $\sigma(d_i)$
1	1792	51.3	1.42	0.20	1.42	0.20
2	5723	76.6	3.02	0.27	4.45	0.17
3	8871	42.7	4.54	0.33	8.99	0.17
4	19835	66.8	∞	--	∞	--

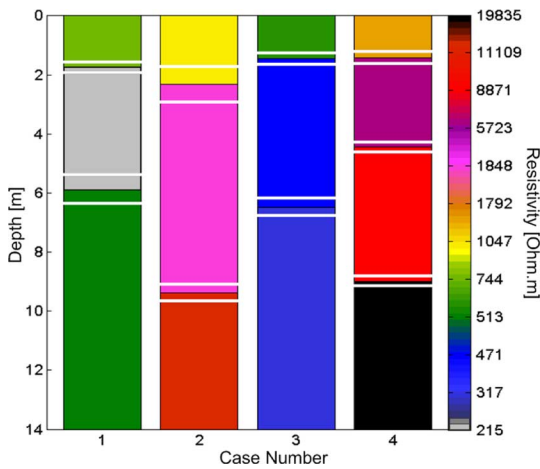


Fig. 11. Visualization of the four stratifications studied (layers mean depths, corresponding SSD, and layers mean resistivities by color scale).

surface depth. The left vertical axis represents the depth scale and the right vertical color scale represents the resistivity.

Table V presents the minimum and maximum depths of the lower boundary surface of each layer, for the four cases, as found by Wenner’s procedure. The analysis of Table V and Fig. 11 results can be useful to identify the adequate depth for the deployment of a ground grid.

Results from Table V and Fig. 11 are merged in one single graphic in Fig. 12, where the stratification for case I is illustrated as an example. This form of presenting horizontal stratification data enables the identification of possible depths where soil with resistivity ρ_i can be found with a given probability.

F. Discussion of Results

It is observed in Figs. 8 and 9 that in some regions of the area, the first layer vanishes. For a better visualization, the figure for case II is redrawn in Fig. 13, and these regions are identified

TABLE V
MINIMUM AND MAXIMUM DEPTH VALUES OF EACH LAYER BOTTOM SURFACE

Case	Bottom Surface of Layer	Minimum [m]	Maximum [m]
1	1	0.44	3.10
	2	4.79	7.05
	3	∞	∞
2	1	0.01	5.02
	2	6.91	11.33
	3	∞	∞
3	1	0.01	2.92
	2	3.20	9.59
	3	∞	∞
4	1	0.10	3.10
	2	2.57	6.32
	3	7.07	11.23
	4	∞	∞

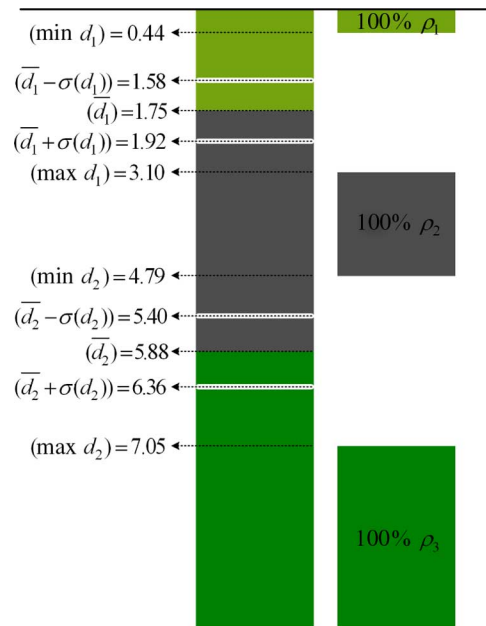


Fig. 12. Distribution of the layers’ depths for case 1 (in meters).

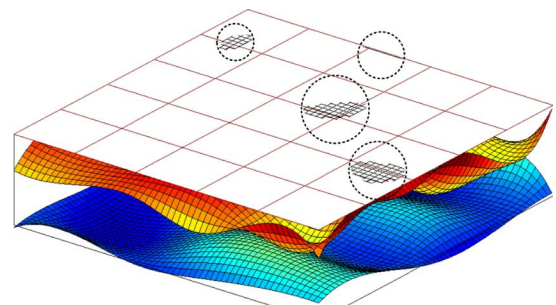


Fig. 13. Case 2—areas where the first layer almost vanishes.

by circles. In locations where the interpolation procedure found negative thickness, this value is truncated to zero.

For a better analysis, the stratification surfaces for each sub-area of case II are visualized without interpolation in Fig. 14. It is verified that for the subareas where the first layer is less

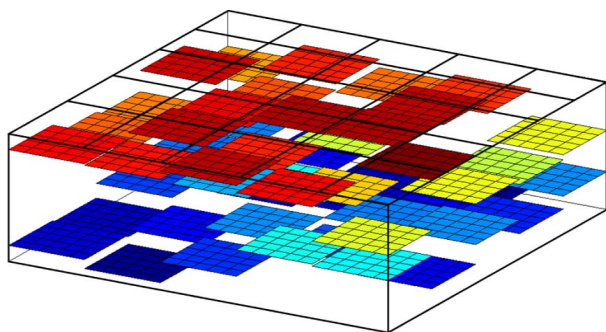


Fig. 14. Second case 3-D noninterpolated stratification surfaces.

than 0.3 m thick and the resistivity gradient between adjacent subareas is high, the interpolation procedure leads to negative thickness, which explains the emerging layers.

The areas of the four cases presented are relatively small and, as a result, its subareas have the same number of layers. This does not necessarily occur when the stratification is performed over a larger terrain. What can happen in a large terrain is that there may be the appearance or disappearance of a given layer of soil, resulting in subareas with a different number of layers. If this was the case with the present study, this phenomenon could be easily identified by analyzing Table V. For instance, if layer one disappears in some subareas, its minimum global depth would be zero.

V. CONCLUSION

Three-dimensional stratification can be considered a *CT scan* (computerized axial tomography) of the soil. This paper presents a 3-D soil stratification methodology which was applied to four different practical stratification cases.

In substation grounding designs, where it is necessary to choose the best location of a grounding grid, usually the design task seeks the best stratification model of the soil. The horizontal layers in the model are considered to have homogeneous resistivities. In the proposed method, since the area to be analyzed is subdivided into subareas, the stratification is sectorized and, thus, the uncertainty about the soil resistivity profile decreases, compared with the traditional stratification process. As a result, by performing 3-D soil stratification, it is possible to identify how deep vertical drivers should be placed, and what the best size of the grounding grid should be in a facility that is being designed.

Another situation where 3-D soil stratification could be advantageous is where the soil has oblique layers. In this case, the traditional stratification process leads to model errors.

Stratification errors in each subarea can arise from two sources, which are: 1) the computational process and 2) the model of horizontal layers does not fit the soil geological formation. In the first case, the numerical errors that are observed are in the range $2.9\% \leq E_T \leq 11.1\%$, which represents reasonable values compared with errors usually accepted in practice.

In the second case, if the error $F(x)$ was large, say, greater than 30%, this would indicate that the soil does not fit the model of horizontal layers due to the existence of blocks of rocks or

vertical cracks, for example. In the analyzed cases, the overall errors are in the mentioned range, which indicates that each obtained stratification matches the soil.

Repeating measurements on subareas where there is a large $F(x)$ error is suggested.

The biggest drawback in applying the proposed method is the need to make a lot of measurements in the field. Depending on the size of the area to be stratified, the number of measures to be undertaken can make the process expensive if it is not automated.

The results of this 3-D stratification method can be presented in table format and visualized in various new graphic ways. Each form of displaying the stratification results has its advantages and disadvantages, depending on the intended purpose.

REFERENCES

- [1] D. H. Griffiths and R. F. King, *Applied Geophysics for Engineers and Geologists: The Elements of Geophysical Prospecting*. Oxford, U.K.: Pergamon, 1981.
- [2] J. L. del Alamo, "A comparison among eight different techniques to achieve an optimum estimation of electrical grounding parameters in two-layered earth," *IEEE Trans. Power Del.*, vol. 8, no. 4, pp. 1890–1899, Oct. 1993.
- [3] E. Orellana, *Prospeccion Geoelectrica por Campos Variables*. Madrid, Spain: Paraninfo, 1974.
- [4] I. T. Dharmadasa, J. R. Lucas, U. Udawatta, and W. D. A. S. Wijayapala, "Determination of earth resistivity profile in multilayer soil," Dept. Elect. Eng., Univ. Moratuwa, Sri Lanka, 2009.
- [5] B. Zhang, X. Cui, L. Li, and J. He, "Parameter estimation of horizontal multilayer earth by complex image method," *IEEE Trans. Power Del.*, vol. 20, no. 2, pp. 1394–1401, Oct. 2005.
- [6] E. D. Sunde, *Earth Conduction Effects in Transmission Systems*. New York: Macmillan, 1968.
- [7] P. J. Lagace, M. H. Vuong, M. Lefebvre, and J. Fortin, "Multilayer resistivity interpretation and error estimation using electrostatic images," *IEEE Trans. Power Del.*, vol. 21, no. 4, pp. 1954–1960, Oct. 2006.
- [8] Y. L. Chow, J. J. Yang, and K. D. Srivastava, "Grounding resistance of buried electrodes in multi-layer earth predicted by simple voltage measurements along earth surface: A theoretical discussion," *IEEE Trans. Power Del.*, vol. 10, no. 2, pp. 707–715, Apr. 1995.
- [9] W. P. Calixto, L. Martins Neto, M. Wu, and K. Yamanaka, "Parameter estimation of a horizontal multilayer soil using genetic algorithm," *IEEE Trans. Power Del.*, vol. 25, no. 3, pp. 1250–1257, Jul. 2010.
- [10] P. J. Lagace, J. Fortin, and E. D. Crainic, "Interpretation of resistivity sounding measurement in n-layer soil using electrostatic images," *IEEE Trans. Power Del.*, vol. 11, no. 3, pp. 1349–1354, Jul. 1996.
- [11] W. P. Calixto, L. Martins Neto, M. Wu, H. J. Kliemann, S. S. Castro, and K. Yamanaka, "Calculation of soil electrical conductivity using a genetic algorithm," *Comput. Electron. Agricult.*, vol. 71, pp. 1–6, 2010.
- [12] *Recommended Practice for Grounding of Industrial and Commercial Power Systems*, IEEE Standard 142-1991.
- [13] *Guide for Measuring Earth Resistivity, Ground Impedance and Surface Potentials of a Ground System*, IEEE 81:1983.
- [14] F. A. Wenner, "Method of measuring earth resistivity," *Bull. Nat. Bureau Standards*, vol. 12, 1916.
- [15] P. Neittaanmäki, M. Rudnicki, and A. Savini, *Inverse Problems and Optimal Design in Electricity and Magnetism*. New York: Oxford Sci., 1996.
- [16] A. Kirsch, *An Introduction to the Mathematical Theory of Inverse Problems Applied Mathematical Sciences*. Berlin, Germany: Springer-Verlag, 1996.
- [17] S. J. Pirson, *Geologic Well Log Analysis*. Houston, TX: Gulf, 1963.
- [18] F. Herrera and M. Lozano, "Gradual distributed real-coded genetic algorithms," *IEEE Trans. Evol. Comput.*, vol. 4, no. 1, pp. 43–63, Apr. 2000.
- [19] Z. Michalewicz, *Genetic Algorithms+Data Structures=Evolution Programs*. New York: Springer, 1992.
- [20] T. Back, *Evolutionary Algorithms in Theory and Practice: Evolution Strategies Evolutionary Programming Genetic Algorithms*. London, U.K.: Oxford Univ. Press, 1996.

- [21] W. P. Calixto, M. Wu, A. A. R. de Sá, A. Cardoso, C. F. R. L. Antunes, A. J. Alves, and L. Martins Neto, "Methodology for tridimensional soil stratification," in *Proc. Int. Conf. Power Electron. Intell. Transport. Syst.*, 2010. [Online]. Available: <http://cpfd.cnki.com.cn/Article/CPFDTOTAL-ZNXX201011019024.htm>
- [22] K. Weltner, J. Grosjean, W. J. Weber, and P. Schuster, *Mathematics for Physicists and Engineers: Fundamentals and Interactive Study Guide*. Berlin, Germany: Springer-Verlag, 2009.



Wesley Pacheco Calixto (M'09) received the B.Sc. degree in physics and M.Sc. degree in electrical engineering from the Federal University of Goiás, Goiania Goiás, Brazil, in 2001 and 2008, respectively, and the D.Sc. degree in electrical engineering from the University of Uberlândia, Uberlândia, Brazil, in 2012.

He was a Professor at the Federal Institute of Goiás (IFG). He works on projects for the development and research into electric grounding systems at the Federal University of Uberlândia, Uberlândia, and at the Institute of Systems and Robotics, University of Coimbra, Coimbra, Portugal. His research interests include electrical machinery, electric grounding systems, mathematical modeling, and optimization.



A. Paulo Coimbra (M'96) received the B.Sc. and Ph.D. degrees in electrical engineering from the University of Coimbra, Coimbra, Portugal, in 1985 and 1996, respectively.

He has been an Assistant Professor in the Department of Electrical and Computer Engineering, University of Coimbra, since 1996. He is a Researcher in the Institute of Systems and Robotics (ISR), University of Coimbra. His research interests include biped robotics, hyper-redundant robots, vision-based robot navigation, electromagnetic compatibility, and finite-element method electromagnetic and thermal analysis.



Bernardo Alvarenga received the B.Sc. degree in electrical engineering from the University of Brasília, Distrito Federal, Brazil, in 1990, the M.Sc. degree in electrical engineering from the Federal University of Uberlândia, Uberlândia, Brazil, in 1993, and the D.Sc. degree in electrical engineering from the University of São Paulo, São Paulo, Brazil, in 2004.

Since 1994, he has been Adjoint Teacher in electrical engineering undergraduate courses and a Researcher with the Electrical and Computer Engineering School, Federal University of Goiás, Goiania, Brazil. His main areas of interest include rotating electrical machines, linear electrical machines, and analysis by numerical methods.



Jose Paulo Molin received the B.Sc. degree in agricultural engineering from the Federal University of Pelotas, Rio Grande do Sul, Brazil, in 1983, the M.Sc. degree in agricultural engineering from the University of Campinas, Campinas, Brazil, in 1991, and the Ph.D. degree in agricultural engineering from the University of Nebraska, Lincoln, in 1996.

Currently, he is an Associate Professor at the University of São Paulo, São Paulo, Brazil. He has experience in agricultural engineering, with an emphasis on machinery and agricultural implements, mainly in the following areas: precision agriculture, spatial variability, sensors, yield maps, Global Navigation Satellite Systems, localized application of inputs, planting, fertilizing, and harvesting.

Dr. Molin received the Young Scientist Award in 1996 with work associated with the doctoral thesis.



Alexandre Cardoso received the B.Sc. degree in electrical engineering from the Federal University of Uberlândia, Uberlândia, Brazil, in 1987, and the M.Sc. degree in electrical engineering, and Ph.D. degree in electrical engineering from the Polytechnic University of São Paulo, São Paulo, Brazil, in 1991 and 2002, respectively.

Currently, he is Associate Professor at the Federal University of Uberlândia, and Coordinator of the Graduate Program in Electrical Engineering (M.Sc. and Ph.D. programs). He has experience in electrical engineering and computer engineering, with an emphasis on software engineering and computer graphics, acting on the following topics: virtual reality, augmented reality, education, virtual environments, human-computer interfaces, and information.



Luciano Martins Neto received the B.Sc. degree in electrical engineering from the Engineer School of Lins, São Paulo, Brazil, in 1971, and the M.Sc. and Ph.D. degrees from the EESC—São Paulo University (USP), São Paulo, Brazil, in 1976 and 1985, respectively.

He works on research-and-development projects in electrical grounding systems at the Electrical Center of Goiás-CELG. His field of interest and activities include electric machinery and electric grounding systems. Currently, he is a Professor in the Electrical Engineering Department, Federal University of Uberlândia, Uberlândia, Brazil.